

Cite this: *Nanoscale Adv.*, 2025, 7, 7239

# Utilization of waste leather for efficient removal of $\text{Ca}^{2+}$ and $\text{Mg}^{2+}$ in lithium carbonate production via nano-structural adsorption

Pengxiang Zhao,<sup>ID</sup>\*<sup>ab</sup> Jianyu Wei,<sup>ID</sup><sup>c</sup> Fumei Wang,<sup>d</sup> Yang Luo<sup>b</sup> and Luming Yang<sup>\*a</sup>

With the growth of electric vehicles (EVs), the demand for battery-grade lithium carbonate ( $\text{Li}_2\text{CO}_3$ ) is increasing significantly. However, a large part of the available  $\text{Li}_2\text{CO}_3$  is of industrial-grade, either ternary material or lithium iron phosphate ( $\text{Li}_2\text{CO}_3$  is one of the precursors for either ternary material or lithium iron phosphate), which cannot satisfy the requirements for the preparation of cathode. Traditional production of battery-grade  $\text{Li}_2\text{CO}_3$  involves converting industrial-grade lithium carbonate into  $\text{LiHCO}_3$  solution through carbonization using  $\text{CO}_2$ ; the insoluble impurities are then removed by filtering, followed by thermal decomposition. However,  $\text{Ca}^{2+}$  and  $\text{Mg}^{2+}$  are the most difficult impurities to be removed due to their similar characteristics as that of  $\text{Li}^+$ . This study evaluates the use of a vegetable-aldehyde combination tanned leather to filter  $\text{Ca}^{2+}$  and  $\text{Mg}^{2+}$  from a  $\text{LiHCO}_3$  solution utilizing the nano structure of the leather. Results show an effective reduction in  $\text{Ca}^{2+}$  and  $\text{Mg}^{2+}$  concentrations in the  $\text{LiHCO}_3$  solution. When treated with EDTA, the leather can be reused for at least 12 cycles, indicating a cost-effective and sustainable high-quality lithium carbonate production strategy. This study highlights the tanned leather's potential as a reliable filtration medium for lithium-ion battery precursors.

Received 6th August 2025  
Accepted 12th September 2025

DOI: 10.1039/d5na00748h

rsc.li/nanoscale-advances

## 1 Introduction

Battery-grade lithium carbonate ( $\text{Li}_2\text{CO}_3$ ) is an irreplaceable compound used as a precursor for cathode materials in lithium-ion batteries.<sup>1,2</sup> With the growth of electric vehicles (EVs), the demand for battery-grade lithium carbonate ( $\text{Li}_2\text{CO}_3$ ) is increasing significantly. As the primary precursor for lithium-ion battery cathodes, battery-grade lithium carbonate plays a crucial role in battery performance and safety.<sup>3–5</sup> With increasing concerns regarding the safety of lithium-ion batteries, the focus within the lithium chemical industry has shifted toward improving battery safety and reducing impurity levels in cathode materials and their precursors.<sup>6</sup>

Currently, the most common method for producing battery-grade lithium carbonate involves converting industrial-grade or crude lithium carbonate into  $\text{LiHCO}_3$  solution by introducing  $\text{CO}_2$ .<sup>7,8</sup> After filtration, the  $\text{LiHCO}_3$  solution undergoes thermal decomposition to produce  $\text{Li}_2\text{CO}_3$ , which is then subjected to centrifugation, washing, and drying to yield the final product.<sup>9</sup>

In this process, the removal of  $\text{Ca}^{2+}$  and  $\text{Mg}^{2+}$  impurities is typically achieved through a two-step procedure.<sup>10</sup> The first step involves filtering the  $\text{LiHCO}_3$  solution to remove most of the insoluble  $\text{Ca}^{2+}$  and  $\text{Mg}^{2+}$  precipitates.<sup>11</sup> The second step employs ion exchange resins, filtration membranes, or chelating agents to deeply purify the filtered  $\text{LiHCO}_3$  solution by removing residual  $\text{Ca}^{2+}$  and  $\text{Mg}^{2+}$  ions.<sup>12</sup>

Grágeda<sup>13</sup> used a combination of chemical precipitation and ion exchange technologies to remove major impurities such as calcium, magnesium, and sulfates from natural brine. Results showed that the combined use of chemical precipitation and ion exchange resins achieved removal efficiencies as high as 99.93% (for magnesium), 98.93% (for calcium), and 97.14% (for sulfates). Additionally, Chen<sup>14</sup> added sodium carbonate to a sulfate solution to precipitate lithium carbonate ( $\text{Li}_2\text{CO}_3$ ). Then, lithium carbonate was added to water to prepare a lithium carbonate slurry, followed by the addition of  $\text{CO}_2$ . Subsequently, Dowex G 26 resin was used to remove calcium and sodium from lithium carbonate. Milyutin<sup>15</sup> used an inorganic adsorbent and an organic ion exchange resin to remove alkaline earth metal and nonferrous metal ions, thus obtaining high-purity lithium carbonate. However, each of these methods has its advantages and disadvantages in the second step: (i) ion exchange resins effectively remove divalent  $\text{Ca}^{2+}$  and  $\text{Mg}^{2+}$  ions but produce large amounts of waste acids, which are environmentally unfriendly. (ii) Membrane filtration is efficient but costly, and the precipitation of lithium carbonate in the  $\text{LiHCO}_3$  solution can cause blockages in the membrane. (iii) Chelating

<sup>a</sup>National Engineering Laboratory for Clean Technology of Leather Manufacture, Sichuan University, Chengdu, 610000, China. E-mail: ylm11982@126.com

<sup>b</sup>Guangzhou Shiling Leather Goods Industry Research Center Co.Ltd, Guangzhou, 510800, China

<sup>c</sup>School of Materials and New Energy, Ningxia University, Yinchuan, Ningxia 750021, China

<sup>d</sup>School of Materials Science and Engineering, Xihua University, Chengdu 610039, China



agents effectively sequester  $\text{Ca}^{2+}$  and  $\text{Mg}^{2+}$  ions, but their introduction into the mother liquor can disrupt the recycling of the lithium carbonate solution.<sup>16,17</sup> Additionally, most chelating agents contain nitrogen, which can impart an unpleasant odor to the lithium carbonate product. Thus, developing an environmentally friendly and efficient process for the removal of  $\text{Ca}^{2+}$  and  $\text{Mg}^{2+}$  impurities from battery-grade lithium carbonate is of significant importance.

It is known that leather is primarily composed of collagen, which contains a high density of carboxyl ( $-\text{COOH}$ ) and amino ( $-\text{NH}_2$ ) groups.<sup>18–20</sup> The leather goods industry generates substantial amounts of leather waste, mainly as by-products from production processes.<sup>21</sup> Utilizing the carboxyl and amino groups in these leather wastes to adsorb  $\text{Ca}^{2+}$  and  $\text{Mg}^{2+}$  ions from the  $\text{LiHCO}_3$  solution not only holds potential for improving the removal of impurities in lithium carbonate production but also offers an effective means for recycling leather waste, thereby reducing environmental pollution.<sup>22</sup>

In a mechanistic aspect, the native carboxyl ( $-\text{COOH}$ ) and amino ( $-\text{NH}_2$ ) groups present on the molecular chains of both leather collagen and tanning agents take part in the core adsorption mechanism. These functional groups can efficiently and selectively adsorb and remove divalent metal ions, such as calcium ( $\text{Ca}^{2+}$ ) and magnesium ( $\text{Mg}^{2+}$ ), from the solution through electrostatic attraction and complexation.

In this study, the feasibility of using leather waste for the removal of calcium and magnesium ions is demonstrated. This study demonstrates the feasibility of utilizing leather waste for the removal of calcium and magnesium ions. Specifically, it investigates the ion-removal performance of leather tanned with various tanning agents in a  $\text{LiHCO}_3$  solution, followed by recycling tests to evaluate the reusability of the leather in subsequent calcium and magnesium ion removal cycles.

## 2 Experimental sections

### 2.1 Materials

Black wattle extract that was used for plant tanning was supplied by Jiangxi Gannan Heijingshu Castanopsis Factory. For the aldehyde tanning, glutaraldehyde was purchased from Sigma-Aldrich (USA). The combined plant-aldehyde tanning process utilized a mixture of the previously mentioned plant tannin and glutaraldehyde. Additionally, the goatskins used for tanning were sourced from a local supplier. Other chemicals and solvents required for the process, including formic acid and sodium bicarbonate, were obtained from Sigma-Aldrich (USA) and used without further purification. The commercial industrial-grade lithium carbonate used in this experiment was purchased from Sichuan Lichun Lithium Battery Technology Co., Ltd.

### 2.2 Operation process

The preparation of tanned goatskins is divided into three processes: (i) plant tanning; (ii) aldehyde tanning; and (iii) combined plant-aldehyde tanning. The details of the preparation are in the SI. As illustrated in Fig. 1, the use of leather as

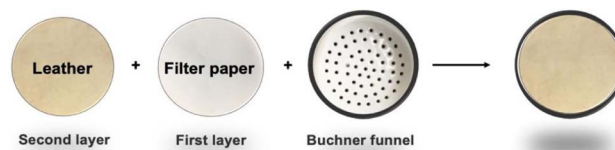


Fig. 1 Scheme of using leather as a filter medium to remove  $\text{Ca}^{2+}$  and  $\text{Mg}^{2+}$  from a lithium bicarbonate solution.

a filter paper for removing calcium and magnesium ions from a lithium bicarbonate solution follows several steps: (i) A standard piece of filter paper is placed as the first filter layer (approximately 7 cm in diameter) at the bottom of a Buchner funnel; (ii) a piece of leather is then placed as the second filter layer (approximately 7 cm in diameter) on top of the filter paper inside the Büchner funnel; (iii) 2000 mL of the lithium bicarbonate solution (with the concentration of  $\text{Li}_2\text{O}$   $20 \text{ g L}^{-1}$ ) is poured into the Büchner funnel; and finally, (iv) the solution is passed through the sheepskin and filter paper, effectively filtering out the calcium and magnesium ions.

### 2.3 Characterization

The FT-IR spectra of the tanned leather samples were recorded using a Perkin-Elmer spectrum-one spectrophotometer. The samples were prepared by mixing 1 wt% tannin with KBr and pressing into pellets. The spectra were collected in the range of  $4000$  to  $450 \text{ cm}^{-1}$  with 32 scans and a resolution of  $4 \text{ cm}^{-1}$ . The mechanical properties, including stress and toughness, of the tanned leather samples were measured using a universal testing machine (Instron). The samples were cut into a standard dumbbell shape, and tensile tests were performed at a cross-head speed of  $10 \text{ mm min}^{-1}$  until failure. The stress and toughness values were calculated from the stress-strain curves. The shrinkage temperature ( $T_s$ ) of the tanned leather samples was determined using a shrinkage tester (SATRA TM 31). The samples were heated at a constant rate, and the temperature at which the leather started to shrink was recorded as the  $T_s$  value. X-ray photoelectron spectroscopy (XPS) was performed using a Kratos Axis Ultra DLD spectrometer with a monochromatic Al  $K\alpha$  source ( $1486.6 \text{ eV}$ ). The spectra were collected at a pass energy of  $160 \text{ eV}$  for survey scans and  $40 \text{ eV}$  for high-resolution scans. The surface composition and chemical states of the elements present in the leather samples were analyzed. Scanning electron microscopy (SEM) was conducted using a JEOL JSM-6510LV microscope. The leather samples were sputter-coated with a thin layer of gold to enhance their conductivity. The microstructure of the tanned leather samples were observed at various magnifications to assess their fiber network and morphology. The isoelectric point of the tanned leather samples was determined by measuring the zeta potential as a function of pH using a zeta potential analyzer (Malvern Zetasizer Nano ZS). The samples were dispersed in water, and the pH was adjusted using hydrochloric acid (HCl) and sodium hydroxide (NaOH) solutions. The pH at which the zeta potential reached zero was recorded as the isoelectric point. The concentration of calcium and magnesium impurity ions was



determined by inductively coupled plasma mass spectrometry (ICP-MS). The ICP process involves nebulizing the solution to form an aerosol that is introduced into the plasma flame, causing the atoms and ions in the solution to become excited. Then, the energy spectral lines and intensities of the excited particles are measured as they transition back to the ground state, thereby determining the content of elements in the product.

## 2.4 Computational details

Density functional theory (DFT) calculations were conducted using the ADF2023 program. The hybrid B3LYP functional was employed in conjunction with an all-electron triple- $\zeta$  Slater basis set augmented by two polarization functions (STO-TZ2P). To account for dispersion forces, Grimme's DFT-D3(BJ) corrections were applied. The bonding energy ( $E_{\text{bond}}$ ) between the metal cation ( $M^{2+}$ ,  $M = \text{Mg}$  and  $\text{Ca}$ ) and the chelating ligands ( $L^{2-}$ ) was obtained by using the following equation:

$$E_{\text{bond}} = E(\text{ML}) - E(\text{M}^{2+}) - E(\text{L}^{2-}) \quad (1)$$

## 3 Results and discussion

### 3.1 Material characterization of goat skin before and after tanning

The stress, toughness and maximum stress temperature of goat skin before and after tanning are well characterized (see Fig. S1–S3). Particularly, by comparing the infrared spectra before and after tanning, key absorption bands that correspond to different chemical groups are observed (Fig. 2). Among these, the amide I (around  $1650 \text{ cm}^{-1}$ ), amide II (around  $1550 \text{ cm}^{-1}$ ), and amide III (around  $1250 \text{ cm}^{-1}$ ) bands are related to amide groups.<sup>23</sup> By analyzing the spectra of differently tanned leather samples (the black line represents raw goat skin, the red line represents TWS, the blue line represents vegetable tanning, and the green line

represents vegetable-aldehyde combination tanning), we can observe the changes in these characteristic absorption bands.

It is obvious that the tanning process increases the amide groups, the intensity of the amide I, amide II, and amide III bands are significantly stronger in the tanned samples (red, blue, and green lines). In the spectra, the absorption intensity at  $1650 \text{ cm}^{-1}$ ,  $1550 \text{ cm}^{-1}$ , and  $1250 \text{ cm}^{-1}$  is indeed higher for the red, blue, and green lines compared with the black line. This indicates that the tanning process introduces more amide groups, and due to the presence of amide groups in the tanning agent, the intensity of these absorption bands is subsequently increased. Thus, comparing the infrared spectra before and after tanning shows that the tanning process indeed increases the number of amide groups in the samples. This is likely due to the formation of new amide bonds between the collagen fibers and tanning agents during the tanning process.

In addition, the XPS analysis of goat skin before and after tanning was conducted (see Fig. S4–S7). Fig. 3 provides valuable insights into the chemical composition and bonding environment of the goat leather samples before and after treatment. For the goat skin without tanning (Fig. 3a), the O 1s spectrum shows two main components: C–O (purple) and C=O (orange). This indicates the presence of both single and double-bonded oxygen atoms, suggesting a relatively balanced mixture of these functional groups. However, for those tanned leathers, including the TWS-tanned (Fig. 3b), vegetable-tanned (Fig. 3c), and vegetable-aldehyde combination tanned (Fig. 3d) leathers, noticeable increases are shown in the C=O component. These results indicate that different tanning processes have various effects on the chemical composition of goat leather, particularly in the formation of carbonyl groups (C=O). The combination of vegetable and acid tanning appears to be the most effective method for enhancing these functional groups in leather.

Besides, compared with the un-tanned goat skin (Fig. 4a), the chemicals used react with the collagen fibers in the tanned

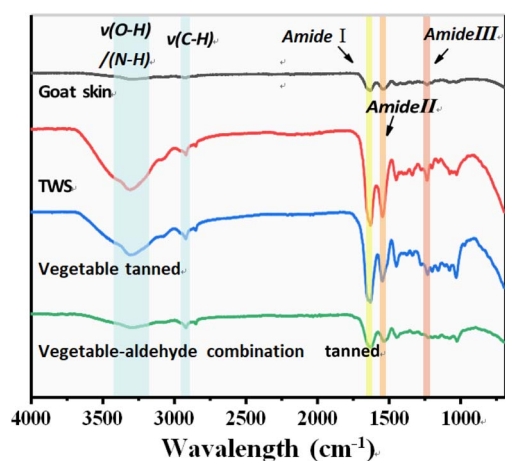


Fig. 2 Comparison of the infrared spectra of different types of tanned leather. (Black line: raw goat skin; red line: TWS tanning; blue line: vegetable tanning; green line: vegetable-aldehyde combination tanning).

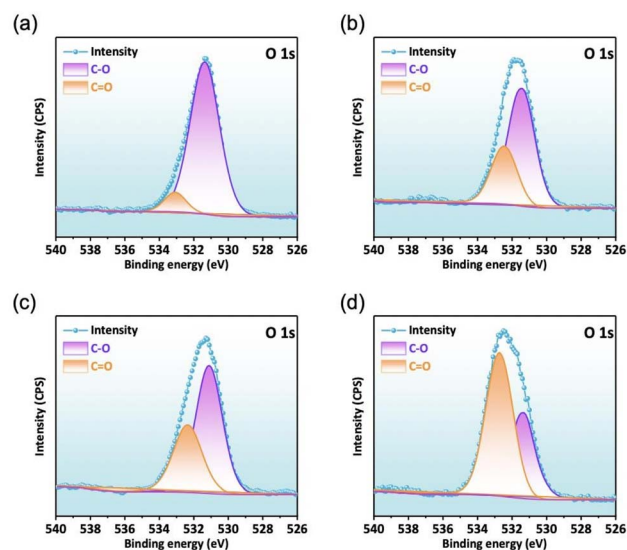


Fig. 3 XPS of C=O bond in different types of leather. (a) Raw goat skin; (b) TWS-tanned; (c) vegetable-tanned; and (d) vegetable-aldehyde combination tanned.



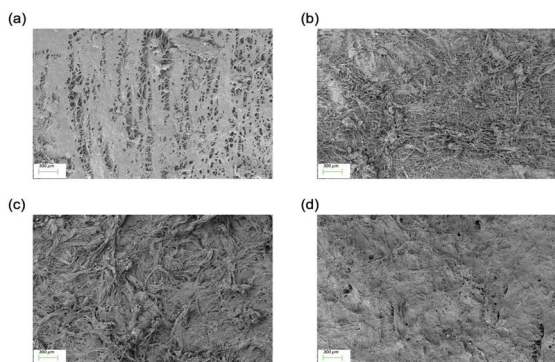


Fig. 4 SEM micrographs of different types of leather. (a) Raw goat skin; (b) TWS-tanned; (c) vegetable-tanned; and (d) vegetable-aldehyde combination tanned.

leather to form a stable cross-linked structure (Fig. 4b–d). This structural change can be observed in the SEM images, which show densely packed fibers and fewer pores.

In summary, the enrichment of amide functional groups (Fig. 3) and the changes in the fiber nanoscale structure of the leather after tanning (Fig. 4) suggest that the tanned leather may have the potential to adsorb calcium and magnesium ions from the solution through coordination and physical adsorption. Specifically, the tanning process increases the number of amide groups in the leather, and these functional groups can form stable coordination bonds with calcium and magnesium ions. Additionally, the tanned leather becomes compact and dense, increasing its surface area, which enables more efficient physical adsorption. Together, these factors may enhance the ability of the tanned leather to adsorb calcium and magnesium ions from solutions.

### 3.2 Removal of $\text{Ca}^{2+}$ and $\text{Mg}^{2+}$ by using untanned and tanned leather

Typically, battery-grade lithium carbonate requires calcium and magnesium ions to be within 50 ppm. This means that in a lithium bicarbonate solution with a  $\text{Li}_2\text{O}$  concentration of  $20 \text{ g L}^{-1}$ , the content of calcium and magnesium should be less than  $2.5 \text{ mg L}^{-1}$ . The removal performance of  $\text{Ca}^{2+}$  and  $\text{Mg}^{2+}$  in  $\text{LiHCO}_3$  solution is conducted as illustrated in Fig. 1. As indicated in Table 1, different types of leather filters are tested for removing  $\text{Ca}^{2+}$  and  $\text{Mg}^{2+}$  ions from a lithium bicarbonate solution. Results show that raw goat skin slightly reduce the ion concentrations, while both TWS-tanned leather and vegetable-

tanned leather brought the levels down to acceptable limits. However, the most effective was the vegetable-aldehyde combination tanned leather, which significantly reduced the ion concentrations to well below the required threshold of  $2.5 \text{ mg L}^{-1}$  for battery-grade lithium carbonate.

Two main reasons could explain the results: (i) the tanning process increases amide groups in leather, creating stable bonds with calcium and magnesium ions. The compact and the nano structure enhance the surface area, improving the physical adsorption and overall efficiency in adsorbing these ions from solutions. Thus, the tanned leather could reduce the ion concentration after filtration. (ii) From the perspective of the isoelectric point (IP), leather's ability to filter  $\text{Ca}^{2+}$  and  $\text{Mg}^{2+}$  depends on the surface charge of the leather. In general, the leather's surface charge is neutral near the IP, leading to low adsorption of these ions. However, when the pH deviates from the IP, the leather surface gains a net charge, enhancing its ability to attract and adsorb oppositely charged ions like  $\text{Ca}^{2+}$  and  $\text{Mg}^{2+}$ . As shown in Fig. 5, the vegetable-aldehyde combination tanned leathers exhibit superior adsorption performance of  $\text{Ca}^{2+}$  and  $\text{Mg}^{2+}$ , which may be attributed to their IP that is far from the pH of the  $\text{LiHCO}_3$  solution. In detail, the leather's superior performance is attributed to its low isoelectric point (IP) of 2.97, which is far from the  $\text{LiHCO}_3$  solution's pH of 9–10. This significant pH difference causes the leather's surface to become strongly negatively charged, creating a powerful electrostatic force that efficiently attracts and captures the

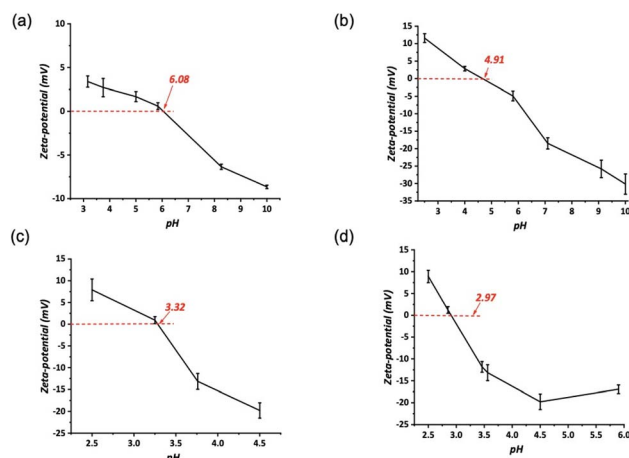


Fig. 5 Zeta potential of different types of leather. (a) Raw goat skin; (b) TWS-tanned; (c) vegetable-tanned; and (d) vegetable-aldehyde combination tanned.

Table 1 Removal of  $\text{Ca}^{2+}$  and  $\text{Mg}^{2+}$  in an  $\text{LiHCO}_3$  solution by different types of leather

Samples	$\text{Ca}^{2+}$ ( $\text{mg L}^{-1}$ )	$\text{Mg}^{2+}$ ( $\text{mg L}^{-1}$ )
Lithium bicarbonate solution (LBS)	7.5	4
LBS filter by raw goat skin	5.5	3.7
LBS filter by TWS tanned leather	2.5	2.2
LBS filter by vegetable-tanned leather	2.4	2.1
LBS filter by vegetable-aldehyde combination tanned leather	1.7	1.2



positively charged  $\text{Ca}^{2+}$  and  $\text{Mg}^{2+}$  ions. This makes the leather a reliable and sustainable filtration medium for producing high-quality lithium carbonate.

### 3.3 Removal amounts of $\text{Ca}^{2+}$ and $\text{Mg}^{2+}$ by using the vegetable-aldehyde combination tanned leather

As mentioned above, the vegetable-aldehyde combination tanned leather is approximately of 7 cm in diameter. In order to evaluate its efficacy in  $\text{Ca}^{2+}$  and  $\text{Mg}^{2+}$  removal, the amounts of  $\text{LiHCO}_3$  (with the concentration of  $7.5 \text{ mg L}^{-1}$   $\text{Ca}^{2+}$  and  $\text{Mg}^{2+}$   $4 \text{ mg L}^{-1}$ ) are varied, and the removal amounts of  $\text{Ca}^{2+}$  and  $\text{Mg}^{2+}$  are measured (Table 2). From the table, it can be observed that with increasing amounts of  $\text{LiHCO}_3$  solution, the removal amounts of  $\text{Ca}^{2+}$  and  $\text{Mg}^{2+}$  by the vegetable-aldehyde combination tanned leather also increase. Initially, for 1 L of  $\text{LiHCO}_3$  solution, the residual concentrations of  $\text{Ca}^{2+}$  and  $\text{Mg}^{2+}$  are  $1.7 \text{ mg L}^{-1}$  and  $1.2 \text{ mg L}^{-1}$ , respectively. As the volume of  $\text{LiHCO}_3$  solution increases to 30 L, the residual concentrations rise to  $2.4 \text{ mg L}^{-1}$  for  $\text{Ca}^{2+}$  and  $2.3 \text{ mg L}^{-1}$  for  $\text{Mg}^{2+}$ .

However, as illustrated above, it is important to note that when the concentrations of  $\text{Ca}^{2+}$  and  $\text{Mg}^{2+}$  exceed  $2.5 \text{ mg L}^{-1}$ , the subsequent thermal decomposition of  $\text{LiHCO}_3$  into  $\text{Li}_2\text{CO}_3$  results in the impurities of  $\text{Ca}^{2+}$  and  $\text{Mg}^{2+}$  in the product, exceeding acceptable standards. Therefore, treating up to 20 L of  $\text{LiHCO}_3$  is considered the safe range for removing  $\text{Ca}^{2+}$  and  $\text{Mg}^{2+}$  using the vegetable-aldehyde combination tanned leather with a 7 cm diameter. This indicates that the vegetable-aldehyde combination tanned leather with a diameter of 7 cm is effective and safe for removing  $\text{Ca}^{2+}$  and  $\text{Mg}^{2+}$  when the volume of  $\text{LiHCO}_3$  solution does not exceed 20 L.

### 3.4 DFT calculations

In order to reuse the tanned leather, the binding of  $\text{Ca}^{2+}$  and  $\text{Mg}^{2+}$  should be removed from the tanned leather. Thus, the chelating ligands, including EDTA, citrate, and tartrate, are used.

As shown in Fig. 6, the bonding energies between the metal cations ( $\text{Mg}^{2+}$  and  $\text{Ca}^{2+}$ ) and the single chelating ligands (EDTA, citrate, and tartrate) are further investigated using DFT calculations. To ensure comparable charge states of the chelating complexes, the deprotonated forms of EDTA ( $[\text{C}_{10}\text{H}_{14}\text{N}_2\text{O}_8]^{2-}$ ), citrate ( $[\text{C}_6\text{H}_5\text{O}_7]^{2-}$ ), and tartrate ( $[\text{C}_4\text{H}_4\text{O}_6]^{2-}$ ) di-anions are used in the calculations. For the Mg series, the EDTA-Mg complex exhibits the lowest bonding energy ( $-698.36 \text{ kcal mol}^{-1}$ ), which is  $67.82 \text{ kcal mol}^{-1}$  and

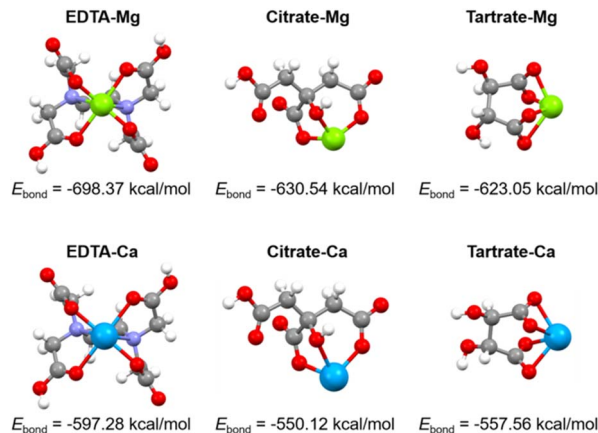


Fig. 6 DFT optimized structures of the magnesium and calcium chelates. The green ball, cyan-blue ball, dark-blue ball, red ball, grey ball and white ball represent Mg, Ca, N, O, C and H atoms, respectively.

$75.31 \text{ kcal mol}^{-1}$  lower than those of the citrate-Mg ( $-630.54 \text{ kcal mol}^{-1}$ ) and tartrate-Mg ( $-623.05 \text{ kcal mol}^{-1}$ ) complexes, respectively. A similar trend is observed for the Ca series, where the bonding energy of the EDTA-Ca complex ( $-597.28 \text{ kcal mol}^{-1}$ ) is significantly lower than those calculated for the citrate-Ca ( $-550.12 \text{ kcal mol}^{-1}$ ) and tartrate-Ca ( $-557.56 \text{ kcal mol}^{-1}$ ) complexes. These results indicate that, compared with citrate and tartrate, the EDTA ligand has a higher ability to chelate with  $\text{Mg}^{2+}$  and  $\text{Ca}^{2+}$  cations. Hence, the EDTA is used to remove the binding of  $\text{Ca}^{2+}$  and  $\text{Mg}^{2+}$  inside the tanned leather.

### 3.5 Re-use of vegetable-aldehyde combination tanned leather

As shown in Fig. 7, the vegetable-aldehyde combination tanned leather can be reused at least 12 times after enrichment with calcium and magnesium. By treating the leather with an EDTA solution, leveraging EDTA's strong binding ability with calcium and magnesium, the leather can be regenerated for continued

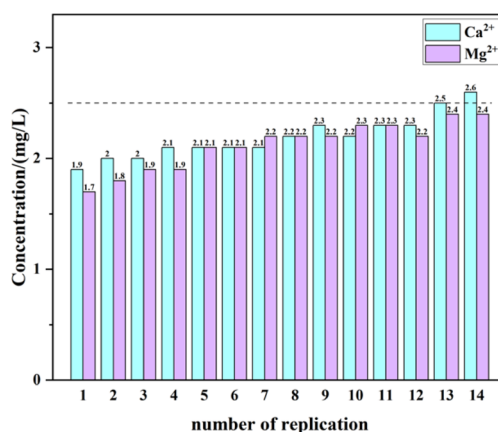


Fig. 7 Recycling of the vegetable-aldehyde combination-tanned leather for the removal of  $\text{Ca}^{2+}$  and  $\text{Mg}^{2+}$ .

Table 2 Residual concentration of  $\text{Ca}^{2+}$  and  $\text{Mg}^{2+}$  in  $\text{LiHCO}_3$  solution after filtration by the vegetable-aldehyde combination tanned leather

Amounts of $\text{LiHCO}_3$ solution	$\text{Ca}^{2+}$ ( $\text{mg L}^{-1}$ )	$\text{Mg}^{2+}$ ( $\text{mg L}^{-1}$ )
1 L	1.7	1.2
5 L	1.7	1.3
10 L	1.9	1.5
20 L	2.1	2.0
30 L	2.4	2.5



use. Fig. 7 illustrates the cyclic reuse of the vegetable-aldehyde combination tanned leather. The figure shows the concentration changes of calcium ions ( $\text{Ca}^{2+}$ ) and magnesium ions ( $\text{Mg}^{2+}$ ) after 14 reuse cycles. It can be observed that during the first 12 reuse cycles the concentration of calcium and magnesium ions remains relatively stable between  $2.1 \text{ mg L}^{-1}$  to  $2.3 \text{ mg L}^{-1}$ , indicating that the leather can be reused at least 12 times. Also, the infrared spectrum in Fig. S8 proved the existence of hydroxyl and amino functional groups.

## Conclusions

In conclusion, this study evaluated the efficacy of using a vegetable-aldehyde combination tanned leather as a filter medium to remove calcium ( $\text{Ca}^{2+}$ ) and magnesium ( $\text{Mg}^{2+}$ ) ions from a lithium bicarbonate  $\text{LiHCO}_3$  solution. Results demonstrated that the vegetable-aldehyde combination tanned leather is highly effective in reducing the concentrations of  $\text{Ca}^{2+}$  and  $\text{Mg}^{2+}$ . Additionally, the used leather could be treated with EDTA solution to chelate and remove the absorbed  $\text{Ca}^{2+}$  and  $\text{Mg}^{2+}$  ions, allowing the leather to be reused at least 12 times. This study found that as the leather can be effectively reused up to at least 12 times, it is a cost-effective and sustainable option. Overall, this study highlights the potential of the vegetable-aldehyde combination tanned leather as a reliable and safe filtration medium for removing  $\text{Ca}^{2+}$  and  $\text{Mg}^{2+}$  ions from  $\text{LiHCO}_3$  solutions, ensuring the production of high-quality lithium carbonate. Last but not least, the reusability of the tanned leather further enhances its applicability and efficiency, presenting promising prospects for resource utilization and new energy industry applications.

## Conflicts of interest

There are no conflicts to declare.

## Data availability

All data supporting the findings of this study are available within the article and its supplementary information (SI) files. Supplementary information is available. See DOI: <https://doi.org/10.1039/d5na00748h>.

## Acknowledgements

The funding of post-doc from Guangzhou and Leather and Leather Goods Industry Research Center and the funding from Aba science and technology bureau (item number: R22ZYZF0003) are gratefully acknowledged.

## Notes and references

1 Z. X. Yuan, Y. Jiang, B. Lin, W. Chen, C. Y. Wang, M. Ding and Z. J. Li, Research progress of ion-initiated in situ generated solid polymer electrolytes for high-safety lithium batteries, *Clin. Chim. Acta*, 2023, **81**, 1064–1080.

- 2 C. F. Wu, C. Wang, J. J. Lu, J. Yuan, P. Zhu and Y. Wang, Crystallization of battery-grade lithium carbonate with high recovery rate via solid-liquid reaction, *Particuology*, 2024, **92**, 95–105.
- 3 W. R. Torres, C. H. D. Nieto, A. PrévotEAU, K. Rabaey and V. Flexer, Lithium carbonate recovery from brines using membrane electrolysis, *J. Membr. Sci.*, 2020, **615**, 118416.
- 4 Z. H. Sun, Y. Chen, C. X. Wang, W. X. Hu, Z. J. Sun, J. Shi and H. Y. Yang, Corrosion behavior of cobalt oxide and lithium carbonate on mullite-cordierite saggars used for lithium battery cathode material sintering, *Materials*, 2023, **16**, 653.
- 5 L. Rosso, L. Alcaraz, O. Rodríguez-Largo and F. A. López, Purification of  $\text{Li}_2\text{CO}_3$  obtained through pyrometallurgical treatment of NMC black mass from electric vehicle batteries, *ChemSusChem*, 2024, e202401722.
- 6 A. Battistel, M. S. Palagonia, D. Brogioli, F. La Mantia and R. Trócoli, Electrochemical methods for lithium recovery: a comprehensive and critical review, *Adv. Mater.*, 2020, **32**, 1905440.
- 7 Z. G. Xu and S. Y. Sun, Preparation of battery-grade lithium carbonate with lithium-containing desorption solution, *Metals*, 2021, **11**, 1490.
- 8 S. Wang, J. X. Li, H. Z. Liu, H. Deng, H. L. Chen, S. H. Sun, H. Y. Chen and H. Yang, Preparation of lithium carbonate by microwave assisted pyrolysis, *Chin. J. Chem. Eng.*, 2022, **52**, 146–153.
- 9 J. J. Lu, C. F. Wu, Y. Wang, J. Yuan and P. Zhu, Preparation of battery-grade lithium carbonate by microbubble enhanced  $\text{CO}_2$  gas-liquid reactive crystallization, *Green Chem.*, 2022, **24**, 9084–9093.
- 10 W. H. Xu, D. F. Liu, L. H. He and Z. W. Zhao, A comprehensive membrane process for preparing lithium carbonate from high Mg/Li brine, *Membranes*, 2020, **10**, 371.
- 11 B. Scrosati and J. Garche, Lithium batteries: Status, prospects and future, *J. Power Sources*, 2010, **195**, 2419–2430.
- 12 C. Quintero, S. O'Brien, R. I. Jeldres, P. Parada, L. Flores, R. Cortes, A. Zuniga and M. Grageda, Development of a co-precipitation process for the preparation of magnesium hydroxide containing lithium carbonate from Li-enriched brines, *Hydrometallurgy*, 2020, **198**, 105515.
- 13 M. Grágeda, A. González, M. Grágeda and S. Ushak, Purification of brines by chemical precipitation and ion-exchange processes for obtaining battery-grade lithium compounds, *Int. J. Energy Res.*, 2018, **42**, 2386–2399.
- 14 W. S. Chen, C. H. Lee and H. J. Ho, Purification of lithium carbonate from sulphate solutions through hydrogenation using the Dowex G26 resin, *Appl. Sci.*, 2018, **8**, 2252.
- 15 V. V. Milyutin, N. A. Nekrasova, V. V. Rudskikh and T. S. Volkova, Preparation of high-purity lithium carbonate using complexing ion-exchange resins, *Russ. J. Appl. Chem.*, 2020, **93**, 549–553.
- 16 M. Zhou, Preparation of battery grade  $\text{Li}_2\text{CO}_3$  from defective product by the carbonation-decomposition method, *Cryst. Res. Technol.*, 2023, **58**, 2200112.
- 17 Z. H. Xu, P. Yu, Z. Liu, Z. Q. Li, F. Zhang, J. C. Yu and R. Zhou, Systemic and direct production of battery-grade lithium



- carbonate from a saline lake, *Ind. Eng. Chem. Res.*, 2014, **53**, 16502–16507.
- 18 F. Yang, Y. W. Zeng, Y. L. Long, H. X. Ding and N. Li, Research recap of membrane technology for tannery wastewater treatment: a review, *Collagen Leather*, 2023, **5**, 132.
- 19 L. Muthukrishnan, Nanotechnology for cleaner leather production: a review, *Environ. Chem. Lett.*, 2021, **19**, 2527–2549.
- 20 V. Muralidharan, S. Palanivel and M. Balaraman, Turning problem into possibility: A comprehensive review on leather solid waste intra-valorization attempts for leather processing, *J. Clean. Prod.*, 2022, **367**, 133021.
- 21 J. Z. Ma, N. Yang, J. B. Shi and X. Y. Yang, Tailoring the structure of layered double oxide for enhancing adsorption of anionic chemicals on collagen fibers in chrome-free leather processing, *Clean Technol. Environ. Policy*, 2022, **24**, 2947–2955.
- 22 M. Ayele, K. Worku, A. Ayele, O. Adewumi, A. Mengesha, S. Ayele and A. Abebe, A review on utilization routes of the leather industry biomass, *Adv. Mater. Sci. Eng.*, 2021, **2021**, 1503524.
- 23 P. Narayanan and S. K. Janardhanan, An approach towards identification of leather from leather-like polymeric material using FTIR-ATR technique, *Collagen Leather*, 2024, **6**, 145.

